

# Intricate Relations Among Particle Collision, Relative Motion and Clustering in Turbulent Clouds: Computational Observation and Theory.

Ewe-Wei Saw<sup>1,2</sup> and Xiaohui Meng<sup>1</sup>

<sup>1</sup>School of Atmospheric Sciences and Guangdong Province Key Laboratory for Climate Change and Natural Disaster Studies, Sun Yat-Sen University, Zhuhai, China

<sup>2</sup>Ministry of Education Key Laboratory of Tropical Atmosphere-Ocean System, Zhuhai, China

**Correspondence:** E.-W. Saw (ewsaw3@gmail.com), X. Meng (mengxh7@mail2.sysu.edu.cn)

## Abstract.

Considering turbulent clouds containing small inertial particles, we investigate the effect of particle collision, in particular collision-coagulation, on particle clustering and particle relative motion. We perform direct numerical simulation (DNS) of coagulating particles in isotropic turbulent flow in the regime of small Stokes number ( $St = 0.001 - 0.54$ ) and find that, due to collision-coagulation, the radial distribution functions (RDFs) fall-off dramatically at scales  $r \sim d$  (where  $d$  is the particle diameter) to small but finite values, while the mean radial-component of particle relative velocities (MRV) increase sharply in magnitudes. Based on a previously proposed Fokker-Planck (drift-diffusion) framework, we derive a theoretical account of the relationship among particle collision-coagulation rate, RDF and MRV. The theory includes contributions from turbulent-fluctuations absent in earlier mean-field theories. We show numerically that the theory accurately accounts for the DNS results (i.e., given an accurate RDF, the theory could produce an accurate MRV). Separately, we also propose a phenomenological model that could directly predict MRV and find that it is accurate when calibrated using fourth moments of the fluid velocities. We use the model to derive a general solution of RDF. We uncover a paradox: the past empirical success of the differential version of the theory is theoretically unjustified. We see a further shape-preserving reduction of the RDF (and MRV) when the gravitational settling parameter ( $S_g$ ) is of order  $O(1)$ . Our results demonstrate strong coupling between RDF and MRV and imply that earlier isolated studies on either RDF or MRV have limited relevance for predicting particle collision rate.

## 1 Introduction

The motion and interactions of small particles in turbulence have fundamental implications for atmospheric clouds; specifically, they are relevant to the time-scale of rain formation particularly in warm-clouds (Falkovich et al., 2002; Wilkinson et al., 2006; Grabowski and Wang, 2013) [a similar problem also applies to planet formation in astrophysics (Johansen et al., 2007)]. They are also important for engineers who are designing future, greener, combustion engines, as this is a scenario they wish to understand and control in order to increase fuel-efficiency (Karnik and Shrimpton, 2012). Cloud particles or droplets, due to their inertia, are known to be ejected from turbulent vortices and thus form clusters – regions of enhanced particle-density (Wood et al., 2005; Bec et al., 2007; Saw et al., 2008; Karpińska et al., 2019); this together with droplet collision is of direct relevance for the mentioned applications. Due to the technical difficulty of obtaining extensive and systematic experimental or field data on particle/droplet collision in turbulent cloud, many of the recent studies rely on direct numerical simulation (DNS), examples of which could be found in, e.g., (Onishi and Seifert, 2016; Wang et al., 2008) and reference therein. Up until now, we do not have definitive answers to basic questions such as how to calculate particle collision rate from basic turbulence-particle parameters and what is the exact relation between collision and particle clustering and/or motions, for, as we shall see, our work reveals that collision-coagulation causes profound changes in particle relative velocity statistics and particle clustering, questioning earlier understanding of the problem. The difficulty of this problem is in part related to

the fact that turbulence is, even by itself, virtually intractable theoretically due to its nonlinear and complex nature.

The quest for a theory of particle collision in turbulence started in 1956 when Saffman and Turner (1956) derived a mean-field formula for collision rate of finite size, inertialess, particles. In another landmark work (Sundaram and Collins, 1997), a general relation among collision-rate ( $R_c$ ), particle clustering and mean particle relative radial velocity was presented:  $R_c/(n_1 n_2 V) = 4\pi d^2 g(d) \langle w_r(d) \rangle_*$ , where  $g(r)$  is the particle radial distribution function (RDF),  $w_r$  is the radial component of relative velocity between two particles,  $\langle \cdot \rangle_*$  denotes averaging over particle-pairs,  $\langle w_r(d) \rangle_*$  is the mean radial-component of relative particle velocity (MRV),  $n_i$ 's are global averages of particle number density,  $V$  is the spatial volume of the domain,  $d$  the particle diameter. The remarkable simplicity of this finding inspired a "separation paradigm", which is the idea that one could study the RDF or MRV separately (which are technically easier), the independent results from the two may be combined to accurately predicts  $R_c$  (an idea that we subsequently challenge). Another work of special interest here is the drift-diffusion model by Chun et al. (2005) (hereafter: CK theory) (note: there are other similar theories (Balkovsky et al., 2001; Zaichik and Alipchenkov, 2003)). The CK theory, derived for non-colliding particles in the limit of vanishing particle Stokes number  $St$  (a quantity that reflects the importance of the particle's inertia in dictating its motion in turbulence), correctly predicted the power-law form of the RDF (Reade and Collins, 2000; Saw et al., 2008) and have seen remarkable successes over the years including the accurate account of the modified RDF of particles interacting electrically (Lu et al., 2010) and hydrodynamically (Yavuz et al., 2018).

Here, we first present results on RDF and MRV for particles undergoing collision-coagulation<sup>1</sup>. The data is obtained via direct numerical simulation (DNS), which is the gold-standard computational method in terms of accuracy and completeness for solving the most challenging fluid dynamics problem, i.e., turbulent flows. It is worth noting that the focus of our work is on the fundamental relationship between collision, RDF and MRV, and to highlight differences from the case with non-colliding particles (Chun et al., 2005). To that end, we have designed the DNS to have an idealized setup similar to what was done in (Chun et al., 2005), which would allow us to identify without doubt the effects of particle collision-coagulation. As a result, this limits the direct applicability to real systems (these limitations are detailed in Sec. 4.5).

Analysis of the DNS results is followed by a theoretical account of the relations between collision-rate, RDF and MRV which includes mean-field contribu-

tions (Saffman and Turner, 1956; Sundaram and Collins, 1997) and contributions from turbulent fluctuations (absent from earlier theories (Saffman and Turner, 1956; Sundaram and Collins, 1997)). The theory is derived from the Fokker-Planck (drift-diffusion) framework first introduced in the CK theory (Chun et al., 2005). We shall see that the main effect of collision-coagulation is the enhanced asymmetry in the particle relative velocity distribution<sup>2</sup> and that this leads to nontrivial outcomes.

## 2 Direct Numerical Simulation (DNS)

To observe how particle collision-coagulation affects RDF and MRV, we performed direct numerical simulation (DNS) of steady-state isotropic turbulence embedded with particles of finite but sub-Kolmogorov size. We solve the incompressible Navier-Stokes Equations (Eq. (1)) using the standard pseudo-spectral method (Rogallo, 1981; Pope, 2000; Mortensen and Langtangen, 2016) inside a triply periodic cubic-box.

$$\begin{aligned} \frac{\partial \mathbf{u}}{\partial t} + \mathbf{u} \cdot \nabla \mathbf{u} &= -\frac{1}{\rho} \nabla p + \nu \nabla^2 \mathbf{u} + \mathbf{f}(\mathbf{x}, t), \\ \nabla \cdot \mathbf{u} &= 0, \end{aligned} \quad (1)$$

where  $\rho, p, \nu, \mathbf{f}$  are the fluid mass-density, pressure, kinematic viscosity, imposed forcing respectively. The velocity field is discretized on a  $256^3$  grid. Aliasing resulting from Fourier transform of truncated series is removed via a 2/3-dealiasing rule (Rogallo, 1981). A statistically stationary and isotropic turbulent flow is achieved by continuously applying random forcing to the lowest wave-numbers until the flow's energy spectrum is in steady-state (Eswaran and Pope, 1988). The 2nd-order Runge-Kutta time stepping was employed. Further details of such a standard turbulence simulator can be found in, e.g., Pope (2000), Rogallo (1981) and Mortensen and Langtangen (2016). The accuracy of DNS for turbulent flows have been experimentally validated for decades (see, e.g., the compilation of results in (Pope, 2000)).

Particles in the simulations are advected via a viscous Stokes drag force (Maxey and Riley, 1983):

$$d\mathbf{v}/dt = (\mathbf{u} - \mathbf{v})/\tau_p,$$

where  $\mathbf{u}, \mathbf{v}$  are the local fluid and particle velocity respectively,  $\tau_p$  is the particle inertia response time, defined as  $\tau_p = \frac{1}{18}(\rho_p/\rho - 1)(d^2/\nu)$ , where  $\rho_p$  is the particle mass-density and  $d$  is the particle diameter. As mentioned, this work focuses on the fundamental relationship between collision-coagulation, RDF and MRV, as well as on addressing the validity of the theory (to be described). It is thus, beneficial to keep the DNS setting idealized (and in the regime relevant for

<sup>1</sup>Coagulation is, in a sense, the simplest outcome of collision. In the sequel we shall argue that the major qualitative conclusions of our work also apply to cases with other collisional outcomes.

<sup>2</sup>In the collision less case, the asymmetry is much weaker and is related to viscous dissipation of energy in turbulence (Pope, 2000).

the theory) for the sake of clarity when interpreting results. To that end, the DNS does not include inter-particle hydrodynamic interactions (HDI) and gravitational settling, nor does it consider the effects of temperature-, humidity-variation and phase transitions. Such practice is not uncommon in studies designed to isolate and address fundamental issues related to particles dynamics in turbulence, examples that are closely related to the current setup and/or problem include (Sundaram and Collins, 1997; Chun et al., 2005; Bec et al., 2007; Salazar et al., 2008; Wang et al., 2008; Woittiez et al., 2009; Voßkuhle et al., 2013). However, such an approach certainly limits the direct applicability of our results to some realistic problems in the atmosphere, these limitations will be detailed in Sec. 4.5, where a discussion of the effects of gravity and HDI is also given.

In this context, the particle Stokes number, defined as  $\tau_p/\tau_\eta$  where  $\tau_\eta$  is the Kolmogorov time-scale, could be expressed as  $St = \frac{1}{18}(\rho_p/\rho - 1)(d/\eta)^2$ , where  $\eta$  is the Kolmogorov length-scale. Time-stepping of the particle motion is done using a 2nd-order modified Runge-Kutta method with "exponential integrator" that is accurate even for  $\tau_p$  much smaller than the fluid's time-step (Ireland et al., 2013). The particles introduced into the simulation are spherical and are of the same size, the initial number of particles is  $10^7$  and they are randomly distributed in space. Particles collide when their volumes overlap and a new particle is formed conserving volume and momentum (Bec et al., 2016). We continuously, randomly, inject new particles so that the system is in a steady-state after some time. Statistical analysis is done at steady-state on monodisperse particles (i.e., particles with the same  $St$ ). Experimental validation of the accuracy of such particle simulating scheme in DNS could be found in Salazar et al. (2008); Saw et al. (2012b, 2014); Dou et al. (2018).

Values of key parameters of the DNS are given in Table 1. Values of other parameters and further details could be found in (Supplements).

### 3 Elements of the Drift-Diffusion Theory

As described in (Chun et al., 2005), in the limit of  $St \ll 1$ , particle motions are closely tied to the fluid velocity and, to leading order, completely specified by the particle position and fluid velocity gradients. We consider the Fokker-Planck equation which is closed and deterministic (see, e.g., Appendix J in (Pope, 2000)):

$$\frac{\partial P}{\partial t} + \frac{\partial(W_i P)}{\partial r_i} = 0, \quad (2)$$

where  $P \equiv P(r_i, t | \Gamma_{ij}(t))$  is the (per volume) probability density (PDF) for a secondary particle to be at vector position  $r_i$  relative to a primary particle at time  $t$ , conditioned

on a fixed and known history of the velocity gradient tensor along the primary particle's trajectory  $\Gamma_{ij}(t)$ ,  $W_i$  is the mean velocity of secondary particles relative to the primary, under the same condition. Note:  $W_i$  is a conditional-average, while  $w_i$  denotes a realization of relative velocity between two particle.

From this, one could derive an equation for  $\langle P \rangle$ :

$$\frac{\partial \langle P \rangle}{\partial t} + \frac{\partial}{\partial r_i} (\langle W_i \rangle \langle P \rangle + \langle W_i P' \rangle) = 0, \quad (3)$$

where  $\langle \cdot \rangle$  implies ensemble averaging over primary particle histories (note:  $\langle W_r \rangle \equiv$  unconditional mean of  $w_r$ , averaged over all particle pairs, i.e., the MRV). This equation, however, is not closed due to the correlation between the fluctuating terms  $W_i$  and  $P' \equiv P - \langle P \rangle$ . The correlation  $\langle W_i P' \rangle$  can be written in terms of a drift flux and diffusive flux (detailed derivation is well described in (Chun et al., 2005)), such that we have:

$$\frac{\partial \langle P \rangle}{\partial t} + \frac{\partial}{\partial r_i} (q_i^d + q_i^D) + \frac{\partial(\langle W_i \rangle \langle P \rangle)}{\partial r_i} = 0, \quad (4)$$

where the drift flux is:

$$q_i^d = - \int_{-\infty}^t \left\langle W_i(\mathbf{r}, t) \frac{\partial W_l}{\partial r'_l}(\mathbf{r}', t') \right\rangle \langle P \rangle(\mathbf{r}', t') dt', \quad (5)$$

and the diffusive flux is:

$$q_i^D = - \int_{-\infty}^t \langle W_i(\mathbf{r}, t) W_j(\mathbf{r}', t') \rangle \frac{\partial \langle P \rangle}{\partial r'_j}(\mathbf{r}', t') dt', \quad (6)$$

where  $\mathbf{r}'$  satisfies a characteristic equation:  $\frac{\partial r'_i}{\partial t'} = W_i(\mathbf{r}', t')$ , with boundary condition  $r'_i = r_i$  at  $t' = t$ .

Finally we note that, since particles are allowed to collide-coagulate in our theory, we use the conventional definition of MRV:  $\langle W_r \rangle \equiv \langle w_r \rangle_*$ . In some works that consider non-colliding (ghost) particles, the conditional mean  $\langle w_r | w_r \leq 0 \rangle_*$  must be used for the purpose of calculating mean collision rate, since there,  $\langle w_r \rangle_* = 0$  due to local isotropy of turbulence (Chun et al., 2005).

### 4 DNS Results, Theory and Discussion

We compute the RDF via  $g(r) = N_{pp}(r) / [\frac{1}{2}N(N-1)\delta V_r/V]$ , where  $N_{pp}(r)$  is the number of particle pairs found to be separated by distance  $r$ ,  $\delta V_r$  is the volume of a spherical shell of radius  $r$  and infinitesimal thickness  $\delta r$ ,

Figure 1 shows the RDFs obtained for monodisperse particles of various Stokes numbers and sizes. Two cases ( $St = 0.22$  and  $0.54$ ) are shown in panel-a and two more ( $St = 0.054$  and  $0.001$ ) are shown in panel-b. In this work, we focus on the smaller values of  $St$  since the theory which we

$Re_\lambda$	$\nu$ [dm <sup>2</sup> /s]	$u_{rms}$ [dm/s]	$\epsilon$ [dm <sup>2</sup> /s <sup>3</sup> ]	$\eta$ [dm]	$\tau_\eta$ [s]	$L_c$ [dm]	$d$ [dm]
133	0.001	0.613	0.117	0.00962	0.0925	$2\pi$	$d_*$ or $2d_*$

**Table 1.** Values of the parameters in the DNS. (Note: dm = decimeter). From the left, we have the Taylor-scale Reynolds number, kinematic viscosity of the fluid, root-mean-square of fluid velocity, kinetic energy dissipation rate, Kolmogorov length- and time-scale, length of the simulation cube and particle diameters considered. We have introduced  $d_*$  to represent the specific value:  $9.49 \times 10^{-4}$  dm (more details in the text). We choose the units of the length (time) scale in the DNS to be in decimeter (second), such that  $\nu$  is nearly its typical value in the atmosphere.

shall consider is also only applicable in the  $St \ll 1$  regime. However, we have included the  $St = 0.54$  case to demonstrate that the observations to be described extends also to finite  $St$ . In all cases, except one, the particles are of the same size  $d = d_*$ , where  $d_*$  represents the specific value of  $d_* = 9.49 \times 10^{-4}$  dm, chosen so that the particle sizes are about  $O(0.1)$  times the Kolmogorov scale ( $\eta$ ), thus allowing us to still observe a regime ( $3d \lesssim r \lesssim 30\eta$ ) of power-law RDFs. To show the effect of changing particle size, panel-a also includes a case of  $St = 0.54, d = 2d_*$  for comparison. Looking at panel-a, apart from the apparent power-law behavior of the RDFs at intermediate values of  $r$ , the most striking feature of these RDFs for colliding-coagulating particles is that they fall-off dramatically in the  $r \sim d$  regime. This is very different from what was seen in earlier studies of non-colliding particles where  $g(r)$  are simple power-laws (Chun et al., 2005; Saw et al., 2008). We also see that as  $r$  approaches  $d$  the steepness of the curve (see, e.g., the blue-circles) increases as  $g(r)$  drops-off, this and the fact that the abscissa is logarithmic implies that  $\frac{\partial g}{\partial r}$  is increasing exponentially in the process. As a consequence, it is difficult to discern from these plots if the limit of  $g(r)$  at particle contact ( $r \rightarrow d$ ) is still nonzero. This is an important question as  $\lim_{r \rightarrow d} [g(r)] = 0$  implies that the mean-field formula of Sundaram and Collins (1997) has zero contribution towards  $R_C$ ; i.e., collision rate is solely due to turbulent-fluctuations. It is only by re-plotting  $g(r)$  versus  $r-d$  (see insets in Fig. 1), and using a remarkable resolution that is  $10^3$  finer than  $d$ , that we see a convincing trend supporting a finite  $g(r \rightarrow d)$ . Also clear in panel-a is the observation that with changing particle size ( $d$ ) the location of the sharp fall-off merely shifts to where the new value of  $d$  is.

The strong effect of particle collision on the RDF (also on MRV as we shall see later) challenges the validity of the "separation paradigm". We note that similar fall-off of RDF was previously observed (Sundaram and Collins, 1997) but a complete analysis and theoretical understanding were lacking. Also, a study on multiple collisions (Voßkuhle et al., 2013) had hinted at the potential problem with the separation paradigm.

Another observation is that in the power-law regime ( $3d \lesssim r \lesssim 30\eta$ ), the RDFs appear (as expected) as straight-lines with slopes (i.e., power-law exponents) that increase with

$St$  and are numerically consistent with those found for non-colliding particles (see, e.g., (Saw et al., 2012b)).

#### 4.1 Theoretical Account via Drift-Diffusion Theory

To theoretically account for the new findings, we make some derivations that are partially similar to the ones in (Chun et al., 2005), but under a new constraint due to coagulations: At contact ( $r = d$ ), the radial component of the particle relative velocities can not be positive<sup>3</sup>, while with increasing  $r$  the constraint is gradually relaxed. The first consequence of this is that the distribution of the radial component of the relative particle velocity ( $W_r$ ) is highly asymmetric at  $r \approx d$ , i.e., the PDF of positive  $W_r$ 's are very small (this constitutes the "enhanced asymmetry" mentioned earlier). Thus for  $r \approx d$ ,  $\langle W_r \rangle$  must be negative. In Sec. 3, we showed that in the  $St \ll 1$  limit, one could derive a master equation (Eq. 4), reproduced here for clarity:

$$\frac{\partial \langle P \rangle}{\partial t} + \frac{\partial}{\partial r_i} (q_i^d + q_i^D) + \frac{\partial (\langle W_i \rangle \langle P \rangle)}{\partial r_i} = 0,$$

where  $q_i^d$  is the drift flux (of probability due to turbulent fluctuation) defined in (5) and  $q_i^D$  is the diffusive flux defined in (6).

We then expand  $W_i$ ,  $\frac{\partial W_i}{\partial r_l}$  and (consequently) the fluxes as perturbation series with  $St$  as the small parameter (details in (Supplements) or (Chun et al., 2005)). The coagulation constraint affects the values of the coefficients of these series. For the drift flux, the leading order terms (in powers of  $St$ ) are:

$$q_i^d = -\langle P \rangle(r) r_k \int_{-\infty}^t [a_{ik}^{(1)} St + a_{ki}^{(2)} St^2] dt', \quad (7)$$

with  $a_{ik}^{(1)} = \tau_\eta \langle \Gamma_{ik}(t) \Gamma_{lm}(t') \Gamma_{ml}(t') \rangle$  and  $a_{ki}^{(2)} = \tau_\eta^2 \langle \Gamma_{ij}(t) \Gamma_{jk}(t) \Gamma_{lm}(t') \Gamma_{ml}(t') \rangle$ ,  $\Gamma_{ij}$  is the  $ij$ -th component of the fluid's velocity gradient tensor at the particle position (the  $a_{ik}$ 's are thus related to two-time correlations of moments of velocity gradients, Chun et al. (2005) shown that  $a_{ik}^{(2)} \propto \overline{S^2} - \overline{R^2}$ , where  $\overline{S^2}$ ,  $\overline{R^2}$  are the average fluid (strain rate tensor, rotation rate tensor) squared at particle

<sup>3</sup>In other words particles may approach each other (and collide) but they can not be created at contact and then separate.

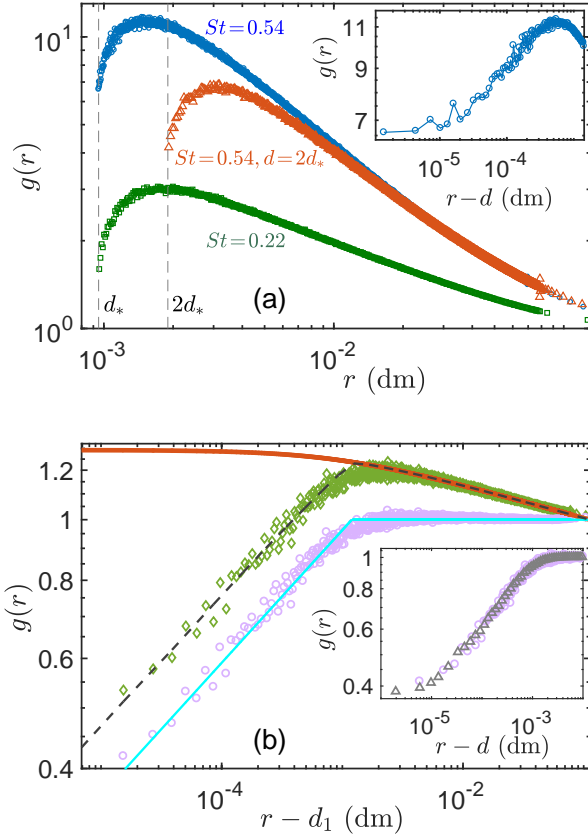


**Figure 1.** RDFs ( $g(r)$ ) of particles that coagulate upon collision. **a)**  $g(r)$  for various cases of Stokes numbers and particle diameters ( $d$ ).  $\square$ :  $St=0.22$ ,  $d=d_*$ ,  $\circ$ :  $St=0.54$ ,  $d=d_*$ ,  $\triangle$ :  $St=0.54$ ,  $d=2d_*$ . All  $g(r)$  drop-off exponentially when  $r \rightarrow d$  (details in text). **Inset:**  $g(r)$  versus  $r-d$  for the  $\circ$  case. It exemplify the fact that  $\lim_{r \rightarrow d} g(r)$  is nonzero. **b)** RDFs versus  $r-d_1$  (where  $d_1=0.99d$ ) for the case of  $St=0.054$ ,  $d=d_*$ .  $\diamond$ : the raw DNS-produced RDF ( $g_{\text{DNS}}(r)$ ). Red-line: power-law fit to  $g_{\text{DNS}}(r)$  (i.e., the  $\diamond$ -plot) in the large- $r$  regime (the fit result is  $0.890r^{-0.0535}$ ). It is equivalent to  $g_s(r)$  in the ansatz  $g_a(r) = g_0(r)g_s(r)$  (i.e., it is the expected RDF for non-colliding particles under the same conditions.  $\circ$ : the compensated RDF, i.e.,  $g_{\text{DNS}}(r)/g_s(r)$  (note:  $g_s(r)$  is the red-line described earlier), this essentially gives us  $g_0(r)$ , which may be understood as a ‘modulation’ on the RDF due to collision-coagulation. Cyan-line: two-piece power-law fits to the compensated RDF (the  $\circ$ -plot) in the small and large  $r-d_1$  regimes respectively (fit results:  $4.17(r-d_1)^{0.212}$ ,  $1.00(r-d_1)^{-2 \times 10^{-4}}$ ), this is an estimate for  $g_0(r)$ . Black-dashed-line:  $g_0(r)g_s(r)$ . (cyan-line  $\times$  red-line), this shows that the ansatz accurately reproduces  $g_{\text{DNS}}(r)$ . **Inset:** RDFs versus  $r-d$ .  $\circ$ : compensated  $g(r)$  for  $St=0.054$ ,  $d=d_*$ , equivalent to the  $\circ$ -plot in the panel’s main figure;  $\triangle$ : compensated RDF for case  $St=0.001$ ,  $d=d_*$ , i.e., finite size, almost zero  $St$  particles (in this case, the compensated and raw RDFs are the identical). This inset suggests that  $g_0(r)$  has negligible  $St$ -dependence.

positions). As explained earlier, coagulation-constraint causes the PDF of relative particle velocities to become highly asymmetric for  $r \sim d$ , thus  $a_{ik}^{(1)}$  is nonzero at this scale. This is very different from the case of non-colliding particles (Chun et al., 2005) where  $a_{ik}^{(1)}$  is always zero due to statistical isotropy. Under the constraint, DNS gives  $\int_{-\infty}^t a_{ik}^{(1)} dt' \approx -0.18 s^{-1}$  and  $\int_{-\infty}^t a_{ki}^{(2)} dt' \approx 2.45 s^{-1}$  (more in (Supplements)). Thus for  $r \sim d$ , the drift flux is negative for large  $St$  but becomes positive<sup>4</sup> when  $St$  is below the value of  $\approx 0.07$ ; and in the limit of  $St \rightarrow 0$ , it is dominated by the first term in (7).

$q_r^D$  is a ‘nonlocal’ diffusion caused by fluctuations and can be estimated using a model that assumes the particle relative motions are due to a series of random uniaxial straining flows (Chun et al., 2005). Chun et al. (2005) showed that, generally,  $q_i^D$  has an integral form (due to nonlocality), and only in the special case where  $g(r)$  is a power-law, may it be cast into a differential form (similar to a local diffusion). In view of the nontrivial  $g(r)$  observed here, we must proceed with the integral form:

$$q_r^D = c_{st} r \times \int d\Omega \int_0^\infty dt_f F(t_f) \int_{d/r}^\infty dR_0 R_0^2 \langle P \rangle (rR_0) f_I(R_0, \mu, t_f),$$

where  $R_0 \equiv r_0/r$  with  $r_0$  as the initial separation distance of a particle pair before a straining event,  $F$  the probability density function for the duration of each event,  $f_I$  is determined by relative prevalence of extensional versus compressional strain events (more details in (Supplements) or (Chun et al., 2005)) and  $\Omega$  is the solid angle for the axis of the straining flow. Note that due to coagulation, the  $R_0$ -integration starts from  $d/r$ . We differ crucially from the CK theory via the introduction of the (positive) factor  $c_{st}$ , which could be shown to equal  $|c_1|$ , where  $c_1$  is the power law exponent of the RDF the particles would have assuming they are non-colliding (details in (Supplements)).

By definition,  $g(r) \equiv \alpha \langle P \rangle$ . Periodic boundaries in our DNS imply that  $\alpha = V$ , (more in (Supplements)). Using this and the fact that the problem has only radial ( $r$ ) dependence, we rewrite (4) as:

$$r^2 \frac{\partial g(r, t)}{\partial t} + \frac{\partial}{\partial r} [r^2 \alpha (q_i^d + q_i^D) + r^2 \langle W_r \rangle g(r, t)] = 0, \quad (8)$$

where the content inside  $[\cdot]$  gives the total flux. For a system in steady-state, the first term in (8) is zero, and upon integrat-

<sup>4</sup>Here a positive  $q_r^d$  merely reflects a deficit in the inward flux of neighboring particles since we find that  $q_r^d + q_r^D$  is always negative.

ing with limits  $[d, r]$ , we have:

$$c_{st} r^3 \int d\Omega \int_0^\infty dt_f F(t_f) \int_{d/r}^\infty dR_0 R_0^2 g(r R_0) f_I(R_0, \mu, t_f) + g(r) [r^2 \langle W_r \rangle - A_\tau r^3] = -R_c^*, \quad (9)$$

where we have identified the total flux at contact ( $r = d$ ) as the negative of the (always positive) normalized collision rate  $R_c^* \equiv R_c / (4\pi[N(N-1)/2]/V)$ , and comparing with (7), we see that:

$$A_\tau \equiv St \int_{-\infty}^t a_{ik}^{(1)} dt' + St^2 \int_{-\infty}^t a_{ki}^{(2)} dt', \quad (10)$$

with the specific values of the  $t'$ -integrals already given above. For clarity, we reiterate that on the left side of Eq. (9), we have the diffusive flux ( $q_r^D$ ), mean-field flux ( $r^2 g(r) \langle W_r \rangle$ ), drift flux ( $q_r^d$ ), while on the right, the total flux is given in terms of the normalized collision rate ( $R_c^*$ ). We note that this equation embodies the full relationship among RDF, MRV and collision rate.

## 4.2 Ansatz and Accuracy of the Theory

Simple analytical solutions to Eq. (9) may be elusive due to its integral nature (a consequence of the non-local diffusive-flux). However, one could gain insights into it and test its accuracy via numerical solutions. To that end, we begin with a simple ansatz for  $g(r)$ , then we curve-fit the ansatz to the DNS-produced RDF ( $g_{\text{DNS}}(r)$ ). This enables us to, firstly, verify that the ansatz could accurately represent  $g_{\text{DNS}}(r)$ , and secondly, obtain a "calibrated" ansatz that is a numerically accurate representation of  $g_{\text{DNS}}(r)$ . We then show that Eq. (9), supplied with the calibrated-ansatz, could numerically predict  $\langle W_r \rangle(r)$  (i.e., the MRV) that agrees well with the DNS-produced MRV. In short, we will show that given a "correct"  $g(r)$ , (9) produces the "correct"  $\langle W_r \rangle(r)$ .

The ansatz has the form  $g_a(r) = g_0(r)g_s(r)$ , with  $g_s(r) = c_0 r^{-c_1}$ , i.e., the RDF form for non-colliding particles (Chun et al., 2005) under the same conditions. As a first order analysis, we let  $g_0$ , which embodies the effects of collision, takes the simplest form that could still capture the main features of the RDFs seen in Fig. 1. Specifically, we let  $g_0(r) = c_{00}(r - d_1)^{c_{10}}$ , where  $c_{00}(r), c_{10}(r)$  are each piecewise constant quantities that switch from their small- $r$  to large- $r$  values at a crossover-scale  $r_c$  (of the order of  $d$ ); i.e.,  $g_0$  is a two-piece power-law of  $r - d_1$ . (Note that our earlier finding of  $g(r \rightarrow d) > 0$  implies that  $d_1 < d$ .)

From a given DNS-produced RDF ( $g_{\text{DNS}}(r)$ ), we first obtain a calibrated  $g_s$  by fitting  $c_0 r^{-c_1}$  to  $g_{\text{DNS}}(r)$  in the power-law regime  $d \ll r \lesssim 10\eta$  (see the red-line in Fig. 1b). Next, we compute the DNS estimate of  $g_0$  via  $g_0^{\text{DNS}} = g_{\text{DNS}}(r)/g_s(r)$  which is essentially a compensated RDF (see the  $\circ$ -plot in Fig. 1b). To get a calibrated  $g_0$ , we then fit the

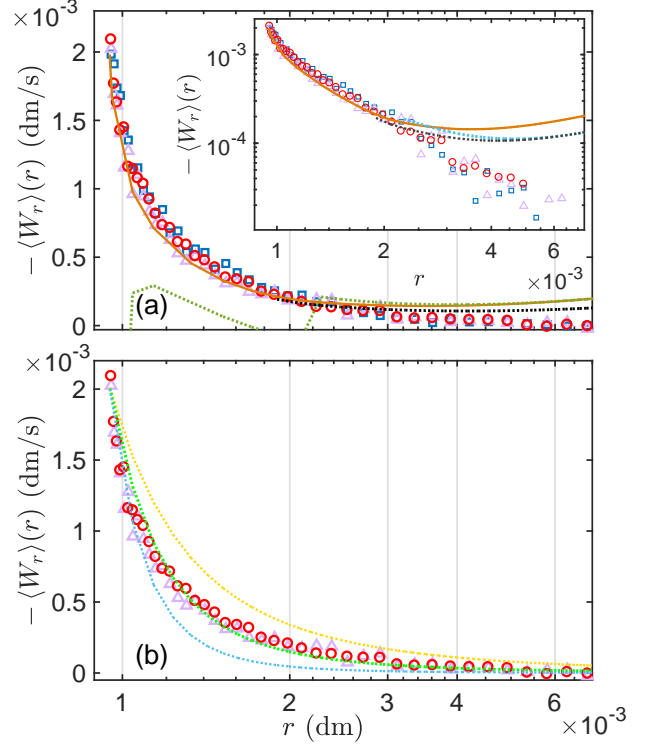


**Figure 2.** Mean radial component of relative velocity (MRV) for particles of specific Stokes numbers and some theoretic-numerical predictions. **a)** Symbols are DNS results with  $\triangle$ :  $St=0.001$ ;  $\circ$ :  $St=0.054$ ;  $\square$ :  $St=0.11$ . The lines are the numerical predictions by the theories (equation (9) or (13)) using the ansatz (details in text). Orange-line:  $\langle W_r \rangle_{r \sim d, St=0.054}^{\text{theory}}$ , i.e., the numerical prediction via the integral version of the theory (Eq. (9)) for the small- $r$  regime ( $r \sim d$ ). Black-line:  $\langle W_r \rangle_{r \gg d, St=0.054}^{\text{theory}}$ , same as the previous but for the large- $r$  regime ( $r \gg d$ ). Green-line: prediction of the differential version of the theory (Eq. (13)) for the  $r \sim d$  regime. **Inset** A repeat of the main figure in log-log axes. Exception: Cyan-line is the prediction of the differential version of the theory, but for the  $r \gg d$  regime. **b)** MRV compared with predictions via the phenomenological model of particle approach angles (Eq. (11) and (12)). DNS results:  $\triangle$ :  $St=0.001$ ;  $\circ$ :  $St=0.054$ . Dotted lines are model predictions of  $\langle W_r \rangle_{St=0}$  using (11) and (12) with variance  $K$  obtained by matching the model's and DNS's transverse-to-longitudinal ratio of structure functions (TLR) of a certain order (from the top, yellow-line: order 2, green-line: order 4, cyan-line: order 6).

general form of  $g_0$  given above to  $g_0^{\text{DNS}}$  (see the cyan-line in Fig. 1b; note that each time, two pieces of power-laws are fitted to one  $g_0^{\text{DNS}}$ , and  $r_c$  results naturally from the intersection of the two). Fig. 1b shows the calibrated ansatz for the case of  $St=0.054$  and verify its accuracy (the red-line is  $g_s(r)$ , the cyan-line is  $g_0(r)$  and the dashed-black-line ( $g_0 \cdot g_s$ ) accurately reproduces  $g_{\text{DNS}}(r)$ ). The inset in Fig. 1b shows that  $g_0^{\text{DNS}}(r)$  (i.e.,  $g_{\text{DNS}}(r)/g_s(r)$ ) is roughly  $St$ -independent for  $St \ll 1$ .

Next, we numerically evaluate the integral in the first term of (9). The  $St \ll 1$  assumption allows us to approximate  $g(r, St)$  inside the integral by its zero- $St$  cousin  $g(r, St \rightarrow 0)$  (Chun et al., 2005). In practice, we replace  $g(r, St)$  with the ansatz fitted to the DNS result of  $g(r, St = 0.001)$ . Next, we use the DNS data to estimate  $A_\tau$ , compute  $R_c^*$  and  $c_{st}$  (for this case, DNS gives  $R_c^* = 9.69 \times 10^{-10} \text{ dm}^3/\text{s}$ ;  $c_{st} = |c_1|$  as mentioned earlier). Finally we use (9) to predict  $\langle W_r \rangle(r)$ .

Comparison of the predicted  $\langle W_r \rangle(r)$  with the ones obtained directly from the DNS is shown in Fig. 2. The prediction shown was made for the case of  $St = 0.054$ , to be compared with its DNS counterpart (the  $\circ$  symbols). (We also show the DNS result for  $St = 0.001$  and  $0.11$  to highlight an observation that  $\langle W_r \rangle(r)$  is almost  $St$ -independent in this small- $St$  regime.) We have shown earlier that for  $r \sim d$ ,  $A_\tau$  is given by (10). However, as stated earlier, as  $r$  increases, the (statistical) asymmetry induced by collision-coagulation gradually becomes subdominant to the isotropy of turbulent-fluctuation. Statistical isotropy implies  $a_{ik}^{(1)} = 0$  (Chun et al., 2005), a fact our DNS data confirm. Thus, for  $r \gg d$ ,  $A_\tau$  equals the order  $St^2$  term in Eq. (10), exactly the same as the results of (Chun et al., 2005) for non-colliding particles. For this reason, we show two versions of the prediction:  $\langle W_r \rangle_{r \sim d}^{\text{theory}}$  and  $\langle W_r \rangle_{r \gg d}^{\text{theory}}$ , which are respectively obtained by setting  $A_\tau$  to its small- $r$  and large- $r$  limits ( $-2.6 \times 10^{-3} s^{-1}$ ,  $7.1 \times 10^{-3} s^{-1}$ ) respectively. The agreement between DNS and the predictions is noteworthy, especially for small  $r$ . At  $r \approx 2d$ , the DNS result shows a weak tendency to first follow the upward trend of  $\langle W_r \rangle_{r \sim d}^{\text{theory}}$  and then drops off significantly at  $r \gtrsim 2.5d$ . The latter is consistent with the fact that  $\langle W_r \rangle_{r \gg d}^{\text{theory}}$  is below  $\langle W_r \rangle_{r \sim d}^{\text{theory}}$ , but the drop is sharper than predicted.

### 4.3 Phenomenological Model of MRV

Alternatively, (9) may be solved for the correct  $g(r)$ , if  $\langle W_r \rangle$  is given. As we are assuming  $St \ll 1$ , particle velocity statistics may be approximated by their fluid counterparts (Chun et al., 2005), i.e., we may replace  $\langle W_r \rangle$  with  $\langle W_r \rangle_{St=0}$ , the latter being the MRV of fluid particles. Hence, if  $\langle W_r \rangle_{St=0}$  is known, it may be used, together with (9), to predict RDF of any finite but small  $St$ . Fig. 2a shows that  $\langle W_r \rangle_{St>0}$  from the DNS do not change significantly for  $St \in [0.001, 0.1]$ , supporting this approach<sup>5</sup>.

Here we provide a simple, first order, model for  $\langle W_r \rangle_{St=0}$ . We limit ourselves to the regime of small particles ( $d \ll \eta$ ) and anticipate that  $\langle W_r \rangle$  is non-trivial (nonzero) only for  $r \sim d$ , a fact observable in Fig. 2a. We also assume that the relative trajectories of particles are rectilinear at such small scales. The coagulation constraint then implies that: in the rest frame of a particle (call it P1), a second particle nearby must move in such a way that the angle ( $\theta$ ) be-

tween its relative velocity and relative position (seen by P1) must satisfy:  $\sin^{-1}(d/r) \leq \theta \leq \pi$ , under the convention of  $\sin^{-1}(x) \in [-\frac{\pi}{2}, \frac{\pi}{2}]$ , (more in (Supplements)). We can thus write (by treating negative and positive  $w_r$  separately, applying the K41 theory (Kolmogorov, 1941) and the bounds on  $\theta$ , details in (Supplements)), for  $St \ll 1$ , that:

$$\begin{aligned} \langle W_r \rangle &\equiv \langle w_r \rangle_* = p_- \langle w_r | w_r < 0 \rangle_* + p_+ \langle w_r | w_r \geq 0 \rangle_* \\ &\approx -p_- \xi_- r + p_+ \xi_+ r \left[ 1 + \frac{\int_{\theta_m}^0 P_\theta^+(\theta') \cos(\theta') d\theta'}{\int_0^{\frac{\pi}{2}} P_\theta^+(\theta') \cos(\theta') d\theta'} \right], \end{aligned} \quad (11)$$

where  $\langle \cdot \rangle_*$  denotes averaging over particle pairs,  $p_+$  ( $p_-$ ) is the probability of a realization of  $w_r$  being positive (negative), and  $P_\theta^+$  is a conditional PDF such that  $P_\theta^+ \equiv P(\theta | w_r \geq 0) \equiv P(\theta | \theta \in [0, \frac{\pi}{2}])$ ,  $\theta_m$  is the lower bound of  $\theta$  described above. For a first order account, we neglect skewness in the distribution of particle relative velocities and set  $p_\pm = 0.5$ . Following Kolmogorov (1941), we have set  $\langle w_r | w_r < 0 \rangle_* = \xi_- r$ , where  $\xi_\pm = C_s \sqrt{\varepsilon}/(15\nu)$ , ( $C_s$  is a Kolmogorov constant, we found  $C_s = 0.76$  by matching  $\xi_- r$  to the first-order fluid velocity structure-function from the DNS).

A simple phenomenological model for  $P(\theta)$  may be constructed using the (statistical) central-limit-theorem by assuming that the angle of approach  $\theta$  at any time is the sum of many random-incremental rotations in the past, thus we write:

$$P(\theta) = N \exp[K \cos(\theta - \mu_\theta)] \sin(\theta), \quad (12)$$

where  $N \exp[\dots]$  is the circular normal distribution, i.e., analog of Gaussian distribution for angular data;  $\sin(\theta)$  results from integration over azimuthal angles ( $\phi$ ). We set  $\mu_\theta = \frac{\pi}{2}$  (neglect skewness in fluid's relative velocity PDF) and obtain  $K$  by matching the transverse to longitudinal ratio of structure functions (TLR) of the particle relative velocities with the ones via the DNS data;  $N$  is determined via normalization of  $P(\theta)$ . Fig. 2b shows the  $\langle w_r \rangle_*$  derived via (11) and (12), using  $K$  calibrated with TLR of 2nd, 4th, 6th order structure functions respectively. The results have correct qualitative trend of vanishing values at large  $r$  that increases sharply as  $r$  approach  $d$ , with the 4th-order's result giving the best agreement with DNS. Currently we have not a satisfactory rationale to single out the 4th-order. The TLR of different orders give differing results may imply that our first-order model may be incomplete, possibly due to oversimplification in (12) or to the inaccuracy of the rectilinear assumption ( $d/\eta$  in the DNS may be insufficiently small).

### 4.4 Differential Version of the Theory, Its Validity and Solution

We now discuss an important but precarious theoretical issue. Chun et al. (2005) clearly showed that the non-local dif-

<sup>5</sup>This is true in the relatively idealized system simulated, but may not apply to the general problem that includes other effects

fusion ( $q_r^D$ ) may be converted, from its general integral form, into a differential version only when the underlying RDF is a simple power-law. However, Lu et al. (2010) and Yavuz et al. (2018), working in two very different scenarios, found that their predictions using the differential form of the theory agree well with experiments, even when the RDFs involved was clearly not power-laws. We shall attempt to remedy this apparent paradox in future work. To examine how well this albeit unjustified method works here, we recast (9) into its differential form (Chun et al., 2005):

$$-\tau_\eta^{-1} B_{nl} r^4 \frac{\partial g}{\partial r} + g(r) [r^2 \langle W_r \rangle - A_\tau r^3] = -R_c^*, \quad (13)$$

where  $B_{nl} = 0.0397$  (this value is computed from our DNS,  $B_{nl}$  is expected to depend on flow characteristics, e.g.,  $R_\lambda$  and  $\tau_\eta$  (more in (Supplements)). Using (13), the same  $g_s g_0$  ansatz, we make another prediction for  $\langle W_r \rangle_{St=0.054}$ , which is plotted in Fig. 2a (dashed green line). This prediction is far from the DNS at  $r \sim d$  but perform as well as the integral version at  $r \gg d$  (the jump in the curve is just an artifact from the kink in the ansatz).

One advantage of (13) is that it allows for a general solution, which we now give, assuming  $\langle W_r \rangle$  is given by (11) & (12):

$$g(r) = \frac{1}{\beta(r)} \left[ \int \beta(r) q(r) dr + C \right], \quad (14)$$

with  $q(r) = R_c^* \tau_\eta / (B_{nl} r^4)$ ,  $\beta(r) = \exp \left[ \int p(r) dr \right]$  and  $p(r) = [A_\tau r - \langle w_r \rangle_*] \tau_\eta / (B_{nl} r^2)$ , (more in (Supplements)).

#### 4.5 Effects of Gravity and Other Limitations

Thus far, we have not considered the effects of gravity on the particles. Here we provide a glimpse on the role of gravity (a detailed analysis is beyond the scope of the present study). In keeping with the scope of current work, we restrict ourselves to the case of monodisperse particle only. For this, we rerun the DNS cases of  $St = 0.054$  and  $0.54$  with gravity (to be compared with the zero-gravity case). The new particle advection equation is:  $d\mathbf{v}/dt = (\mathbf{u} - \mathbf{v})/\tau_p + \mathbf{g}$  (all other details of the DNS remain unchanged). We choose to have the particle settling parameter  $S_g \equiv \tau_p g / u_\eta$  (where  $u_\eta$  is the Kolmogorov velocity scale) be in the range  $O(0.1) - O(1)$  (this is achieved by letting  $|\mathbf{g}| = 10 \text{ dm/s}^2$ ). As a result, the range of  $S_g$  and  $St$  explored here are well aligned with measured values in natural clouds (Siebert et al., 2010). For the case of  $St = 0.054$  ( $S_g = 0.49$ ), we find no discernible difference for both RDF and MRV between the "with gravity" and zero-gravity results (corresponding figures in (Supplements)). For the  $St = 0.54$  ( $S_g = 4.9$ ) case, Fig. 3 shows the effects of gravity on the RDF and MRV. We see that the slope (exponent of  $g(r)$  in the range  $d \ll r < 20\eta$ ) of the RDF in the gravitational case is reduced by about 15% compared to the

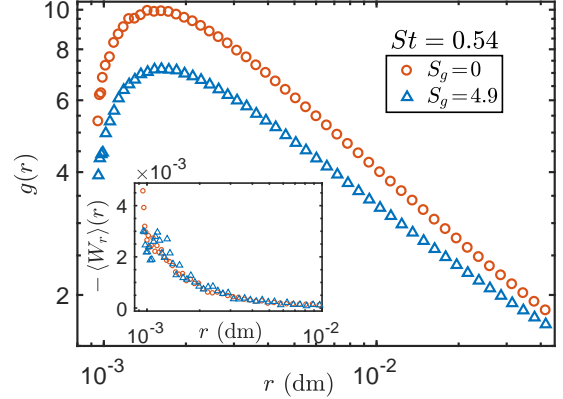


**Figure 3.** RDFs of particles ( $St = 0.54$ ) subject to action of turbulence, collision-coagulation with and without gravity. Circles:  $S_g = 0$  (zero gravity); triangles:  $S_g = 4.9$  (nonzero gravity). The latter shows a reduced slope in the power-law regime, while the shape of the two curves largely similar in the collision regime ( $r \sim d$ ). **Inset** MRVs of the same cases as in the main figure. Gravity weakens the MRV of the particles.

zero-gravity case ( $S_g = 0$ ). However, the shape of the RDF in the collision regime ( $r \sim d$ ) is approximately preserved, suggesting that a construct of the form  $g_{\text{collision}} \times g_{\text{gravity}}$  may be a good first order model for the full RDF (close examination of the compensated RDFs gives substantial support for this idea, details in (Supplements)). These observations imply that as  $S_g$  increase from  $O(0.1)$  to  $O(1)$ , the effects of gravity on RDF grow from negligible to significant but not dominant, the main effect is the reduction of the exponent while the collision related "modulation" ( $g_{\text{collision}}$ ) remains largely intact. The inset of Fig. 3 shows that the MRV is also weakened by gravity, albeit the statistical noise limits the strength of this conclusion. Lastly, It is worth noting that in the complimentary DNS by Woittiez et al. (2009) that included gravity but not actual collisions, much stronger gravitational effect was found on the statistics of bidisperse particles relative to the monodisperse case.

As mentioned, the fundamental focus of our work precludes the DNS and theory from considering a number of complexities relevant to some applications. As a result, this limits the direct quantitative applicability of our results to some realistic problems (e.g., in clouds). Besides gravity, another neglected factor is the hydrodynamic interparticle-force (HDI). Recent works, e.g., Yavuz et al. (2018); Bragg et al. (2022) found that HDI also has strong impact on RDF for  $r \sim d$ . For monodisperse particles with small to moderate  $St$ , HDI is expected to be more important than gravity. While we expect that HDI should not alter the qualitative trend that  $g(r)$  should fall towards a small value at  $r \rightarrow d$  (the same applies to the observed trend of MRV), it is



likely that HDI and collision would affect RDF and MRV in a coupled manner.

Also neglected is the influence of temperature, humidity and vapor-liquid phase transition which are important in the atmospheric clouds. These factors have substantial impact on the polydispersity of small droplets (see, e.g., (Kumar et al., 2012, 2014)). However, for monodisperse statistics considered here, they are likely to play minor roles (they will be more important when future works consider the full polydisperse problem).

One limitation of the theory stems from the assumption of  $St \ll 1$  and its corollary that particle velocity statistics in this regime are  $St$ -independent (Chun et al., 2005), which limits the theory's applicability to real systems. This implies that MRV should be  $St$ -independent in this regime. Our DNS results (spanning two orders of magnitude in  $St$ ) shown in Fig. 2 give some support to the latter. However, unlike the theoretical prediction for MRV of case  $St = 0.054$  (Fig. 2), we have found that the prediction for  $St = 0.11$  is discernibly below the DNS result (figure in (Supplements)). This could be due to the finite  $St$  effect not captured by the theory or other reasons (details in (Supplements)). Hence, a finite  $St$  extension of the theory is desirable to improve its applicability to real systems.

## 5 Conclusions

To conclude, we observed that collision strongly affects the RDF and MRV and imposes strong coupling between them<sup>6</sup>. This challenges the efficacy of a "separation paradigm" and suggests that results from any studies that preclude particle collision has limited relevance for predicting collision statistics. We have presented a theory for particle collision-coagulation in turbulence (based on a Fokker-Planck framework) that explains the above observations and verified its accuracy by showing that  $\langle W_r \rangle$  could be accurately predicted using a sufficiently accurate RDF. The theory accounts for the full collision-coagulation rate which includes contributions from mean-field and fluctuations, and as such, our work complements and completes earlier mean-field theories (Saffman and Turner, 1956; Sundaram and Collins, 1997). We showed that a simple model of particle approach-angles could capture the main features of  $\langle W_r \rangle$  and applied it to derive a general solution for RDF from the differential version of the theory. We uncovered a possible paradox regarding the past empirical successes of the differential drift-diffusion equation (see Sec. 4.4). Further shape-preserving reduction of the RDF and MRV were observed when gravitational settling parameter ( $S_g$ ) is of order  $O(1)$ . Our findings provide new perspectives of particle collision and its relation with clustering and relative motion, which have implications for

atmospheric clouds or generally for systems involving colliding particles in unsteady flows.

*Author contributions.* EWS oversaw the conception and execution of the project. EWS did the theoretical derivations in collaboration with XM. XM and EWS conducted the numerical simulation and data analysis. EWS and XM wrote the article.

*Competing interests.* The authors declared that none of them has any competing interests.

*Acknowledgements.* This work was supported by the National Natural Science Foundation of China (Grant 11872382) and by the Thousand Young Talent Program of China. We thank Jialei Song for helps. We thank Wai Chi Cheng, Jianhua Lv, Liubin Pan, Raymond A. Shaw for discussion and suggestions.

## References

- Arfken, G. B. and Weber, H. J.: Mathematical methods for physicists, 1999.
- Balkovsky, E., Falkovich, G., and Fouxon, A.: Intermittent Distribution of Inertial Particles in Turbulent Flows, *Phy. Rev. Lett.*, 86, 2790, 2001.
- Bec, J., Biferale, L., Cencini, M., Lanotte, A., Musacchio, S., and Toschi, F.: Heavy Particle Concentration in Turbulence at Dissipative and Inertial Scales, *Phy. Rev. Lett.*, 98, 084 502, 2007.
- Bec, J., Ray, S. S., Saw, E. W., and Homann, H.: Abrupt growth of large aggregates by correlated coalescences in turbulent flow, *Physical Review E*, 93, 031 102, 2016.
- Bragg, A. D., Hammond, A. L., Dhariwal, R., and Meng, H.: Hydrodynamic interactions and extreme particle clustering in turbulence, *Journal of Fluid Mechanics*, 933, 2022.
- Chun, J., Koch, D. L., Rani, S. L., Ahluwalia, A., and Collins, L. R.: Clustering of aerosol particles in isotropic turbulence, *J. Fluid Mech.*, 536, 219–251, 2005.
- Dou, Z., Bragg, A. D., Hammond, A. L., Liang, Z., Collins, L. R., and Meng, H.: Effects of Reynolds number and Stokes number on particle-pair relative velocity in isotropic turbulence: a systematic experimental study, *Journal of Fluid Mechanics*, 839, 271–292, 2018.
- Eswaran, V. and Pope, S. B.: An examination of forcing in direct numerical simulations of turbulence, *Computers & Fluids*, 16, 257–278, 1988.
- Falkovich, G., Fouxon, A., and Stepanov, M. G.: Acceleration of rain initiation by cloud turbulence, *Nature*, 419, 151, 2002.
- Grabowski, W. W. and Wang, L.-P.: Growth of cloud droplets in a turbulent environment, *Annual review of fluid mechanics*, 45, 293–324, 2013.
- Ireland, P. J., Vaithianathan, T., Sukheswalla, P. S., Ray, B., and Collins, L. R.: Highly parallel particle-laden flow solver for turbulence research, *Computers & Fluids*, 76, 170–177, 2013.
- Johansen, A., Oishi, J. S., Mac Low, M.-M., Klahr, H., Henning, T., and Youdin, A.: Rapid planetesimal formation in turbulent circumstellar disks, *Nature*, 448, 1022–1025, 2007.

<sup>6</sup>This statement also holds for other types of collisional outcomes (not only for collision-coagulation), but the details of the specific outcomes should be different from the current case.

- Karnik, A. U. and Shrimpton, J. S.: Mitigation of preferential concentration of small inertial particles in stationary isotropic turbulence using electrical and gravitational body forces, *Physics of Fluids*, 24, 073 301, 2012.
- Karpińska, K., Bodenschatz, J. F. E., Malinowski, S. P., Nowak, J. L., Risius, S., Schmeissner, T., Shaw, R. A., Siebert, H., Xi, H., Xu, H., and Bodenschatz, E.: Turbulence-induced cloud voids: observation and interpretation, *Atmospheric Chemistry and Physics*, 19, 4991–5003, <https://doi.org/10.5194/acp-19-4991-2019>, 2019.
- Kolmogorov, A. N.: The local structure of turbulence in incompressible viscous fluid for very large Reynolds numbers, *Dokl. Akad. Nauk SSSR*, 30, 299–303, 1941.
- Kumar, B., Janetzko, F., Schumacher, J., and Shaw, R. A.: Extreme responses of a coupled scalar–particle system during turbulent mixing, *New Journal of Physics*, 14, 115 020, 2012.
- Kumar, B., Schumacher, J., and Shaw, R. A.: Lagrangian mixing dynamics at the cloudy–clear air interface, *Journal of the Atmospheric Sciences*, 71, 2564–2580, 2014.
- Lu, J., Nordsiek, H., Saw, E. W., and Shaw, R. A.: Clustering of Charged Inertial Particles in Turbulence, *Phys. Rev. Lett.*, 104, 184 505, 2010.
- Maxey, M. R. and Riley, J. J.: Equation of motion for a small rigid sphere in a nonuniform flow, *The Physics of Fluids*, 26, 883–889, 1983.
- Mortensen, M. and Langtangen, H. P.: High performance Python for direct numerical simulations of turbulent flows, *Computer Physics Communications*, 203, 53–65, 2016.
- Onishi, R. and Seifert, A.: Reynolds-number dependence of turbulence enhancement on collision growth, *Atmospheric Chemistry and Physics*, 16, 12 441–12 455, <https://doi.org/10.5194/acp-16-12441-2016>, 2016.
- Pope, S. B.: *Turbulent Flows*, Cambridge Univ. Press, Cambridge, UK, 2000.
- Reade, W. C. and Collins, L. R.: Effect of preferential concentration on turbulent collision rates, *Phys. Fluids*, 12, 2530, 2000.
- Rogallo, R. S.: Numerical experiments in homogeneous turbulence, vol. 81315, National Aeronautics and Space Administration, 1981.
- Saffman, P. and Turner, J.: On the collision of drops in turbulent clouds, *Journal of Fluid Mechanics*, 1, 16–30, 1956.
- Salazar, J. P. L. C., de Jong, J., Cao, L., S. H. Woodward, H. M., and Collins, L. R.: Experimental and numerical investigation of inertial particle clustering in isotropic turbulence, *J. Fluid Mech.*, 600, 245–256, 2008.
- Saw, E. W., Shaw, R. A., Ayyalasomayajula, S., Chuang, P. Y., and Gylfason, A.: Inertial Clustering of Particles in High-Reynolds-Number Turbulence, *Phys. Rev. Lett.*, 100, 214 501, 2008.
- Saw, E.-W., Salazar, J. P., Collins, L. R., and Shaw, R. A.: Spatial clustering of polydisperse inertial particles in turbulence: I. Comparing simulation with theory, *New Journal of Physics*, 14, 105 030, 2012a.
- Saw, E.-W., Shaw, R. A., Salazar, J. P., and Collins, L. R.: Spatial clustering of polydisperse inertial particles in turbulence: II. Comparing simulation with experiment, *New Journal of Physics*, 14, 105 031, 2012b.
- Saw, E.-W., Bewley, G. P., Bodenschatz, E., Sankar Ray, S., and Bec, J.: Extreme fluctuations of the relative velocities between droplets in turbulent airflow, *Physics of Fluids*, 26, 111 702, 2014.
- Siebert, H., Gerashchenko, S., Gylfason, A., Lehmann, K., Collins, L., Shaw, R., and Warhaft, Z.: Towards understanding the role of turbulence on droplets in clouds: in situ and laboratory measurements, *Atmospheric research*, 97, 426–437, 2010.
- Sundaram, S. and Collins, L.: Collision statistics in an isotropic particle-laden turbulent suspension. Part 1. Direct numerical simulations, *J. Fluid Mech.*, 335, 75–109, 1997.
- Supplements: See Supplementary Material at XXX. For the ArXiv version, it is attached as Appendix after the References.
- Voßkuhle, M., Lévêque, E., Wilkinson, M., and Pumir, A.: Multiple collisions in turbulent flows, *Physical Review E*, 88, 063 008, 2013.
- Wang, L.-P., Ayala, O., Rosa, B., and Grabowski, W. W.: Turbulent collision efficiency of heavy particles relevant to cloud droplets, *New Journal of Physics*, 10, 075 013, <https://doi.org/10.1088/1367-2630/10/7/075013>, 2008.
- Wilkinson, M., Mehlig, B., and Bezuglyy, V.: Caustic activation of rain showers, *Phys. Rev. Lett.*, 97, 48 501, 2006.
- Woittiez, E. J., Jonker, H. J., and Portela, L. M.: On the combined effects of turbulence and gravity on droplet collisions in clouds: a numerical study, *Journal of the atmospheric sciences*, 66, 1926–1943, 2009.
- Wood, A. M., Hwang, W., and Eaton, J. K.: Preferential concentration of particles in homogeneous and isotropic turbulence, *Int. J. Multiphase Flow*, 31, 1220, 2005.
- Yavuz, M., Kunnen, R., Van Heijst, G., and Clercx, H.: Extreme small-scale clustering of droplets in turbulence driven by hydrodynamic interactions, *Phys. Rev. Lett.*, 120, 244 504, 2018.
- Zaichik, L. I. and Alipchenkov, V. M.: Pair dispersion and preferential concentration of particles in isotropic turbulence, *Phys. of Fluids*, 15, 1776, 2003.

## Supplementary Material

### Further Details of the Direct Numerical Simulation.

The time step in our DNS  $\Delta t$  is 0.001 s. The Courant number is  $C = 0.073$ , (where  $C = \Delta t \left[ \frac{u'}{\Delta x} + \frac{v'}{\Delta y} + \frac{w'}{\Delta z} \right]_{\max}$ ,  $u'$  etc. are r.m.s. velocities,  $\Delta x$  etc. are grid spacings). The normalized maximum wavenumber simulated is  $k_{\max}\eta = 1.2$ . The turbulent flow is sustained by randomly forcing the two lowest nonzero shells of wave numbers. The integral length scale of the turbulent flow is estimated to be  $L = 0.646$  dm.

We study the statistics of monomers only (i.e., the particle of the same size ( $d$ ) that we initially introduce into the system and which we later replenish at a constant rate close to the monomer-monomer collision rate). In this sense, the particle (monomers) are naturally lost from our consideration once they collide and become larger particles. Particles that become much larger ( $St > 21.6$ ) are removed from the DNS at each time step.

### Estimation of Leading Order Terms in the Drift Flux, e.g. $a_{ik}^{(1)}$

Using the DNS data, we estimate, e.g., the value of

$$\int_{-\infty}^t a_{ik}^{(1)} dt' \equiv \int_{-\infty}^t \tau_\eta \langle \Gamma_{ik}(t) \Gamma_{lm}(t') \Gamma_{ml}(t') \rangle dt'.$$

Note: the averaging is done over fluid particles (the theory assumed  $St \ll 1$  limit, such that all velocity statistics are tied to the fluid's), the integrand is non-vanishing only for  $t'$  in the vicinity of  $t - \tau_\eta$  to  $t$  (where the turbulent velocity gradient  $\Gamma_{ij}$  retains correlation), thus this quantity may be approximated as:  $\tau_\eta^2 \langle \Gamma_{ik}(t) \Gamma_{lm}(t) \Gamma_{ml}(t) \rangle$ . As shown in Chun et al. (2005),  $\langle \Gamma_{ik}(t) \Gamma_{lm}(t) \Gamma_{ml}(t) \rangle$  is by definition zero in fully developed turbulence due to the fact that the small-scale statistics of turbulent flows are almost isotropic Kolmogorov (1941). However, the coagulation constraint dictates that at  $r = d$ , such averages must be taken with the condition that only fluid-particle pairs with negative radial velocity ( $w_r < 0$ ) are taken into account (that the inertial particles' motion being tied to the fluid's does not imply that inertial pairs sample the fluid particle pairs' motion uniformly). Under this condition, the DNS data gives  $\tau_\eta^2 \langle \Gamma_{ik}(t) \Gamma_{lm}(t) \Gamma_{ml}(t) \rangle \approx (-0.171 \times 10^{-3} \text{ dm/s})/d_*$ , ( $d_* = 9.49 \times 10^{-4} \text{ dm}$ ); here, it is of value to point out that without such constraint or condition, the result for this quantity from the DNS is two orders of magnitude smaller. Similarly, we found  $\int_{-\infty}^t a_{ki}^{(2)} dt' \approx \tau_\eta^3 \langle \Gamma_{ij}(t) \Gamma_{jk}(t) \Gamma_{lm}(t) \Gamma_{ml}(t) \rangle \approx (2.32 \times 10^{-3} \text{ dm/s})/d_*$ ; for this quantity, the DNS gives roughly the same values with or without the constraint.

### Full Definition of the Function $f_I(R_0, \mu, t_f)$ in the Model for Non-local Diffusive Flux.

Derived in Chun et al. (2005), summarized here (with typo corrected), the diffusive action of the turbulence on the particle-pairs is assumed to consist of a random sequence of uniaxial extensional or compressional flows defined, and:

$$f_I(R_0, \mu, t_f) \equiv f_+ I_+(R_0, \mu, t_f) + f_- I_-(R_0, \mu, t_f),$$

where  $R_0 \equiv r_0/r$ ,  $r_0$  is the initial separation distance of a particle pair before a straining event,  $r$  is the independent variable of the equation for  $g(r)$ ;  $f_+$  and  $f_- \equiv 1 - f_+$  are the fractions of those flows that are extensional and compressional, respectively. Comparing with DNS, Chun et al. (2005) calibrated  $f_+$  and found  $f_+ = 0.188$  (a result we use here).  $I_\pm$  is an indicator function such that it takes the value  $+1$  ( $-1$ ) when a secondary particle leaves (enters) a sphere of radius  $r$  centered on the primary particle, and otherwise zero.  $\mu$  is the cosine of the angle between the axis of symmetry of the straining flow event and the displacement vector between the two particles,  $t_f$  is the lifetime of the event. To obtain a strain rate correlation function that decays exponentially with a characteristic time scale  $\tau_S$ , Chun et al. (2005) set the probability density function for  $t_f$  to be:

$$F(t_f) = \frac{f_s t_f}{\tau_S^2} \exp(-t_f/\tau_S).$$

The indicator function is used to count the net loss of particles from within the sphere over the duration of an (extensional or compressional) event and can be expressed as:

$$I_\pm(R_0, \mu, t_f) = H(1 - R_0)H(R_{f\pm} - 1) - H(R_0 - 1)H(1 - R_{f\pm}),$$

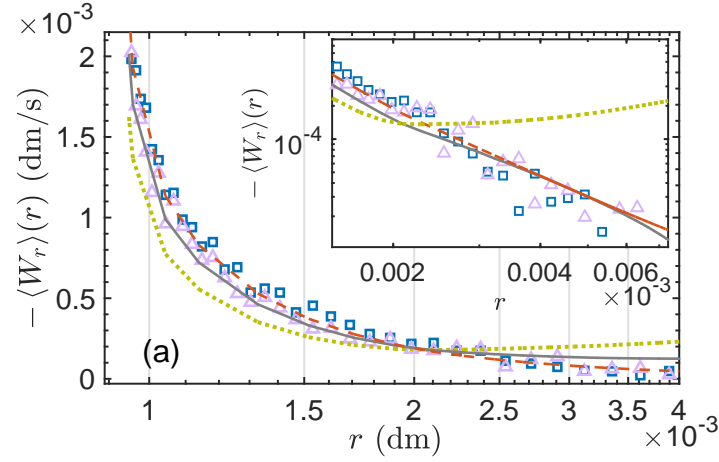


**Figure 11.** MRVs of particles. Triangles: DNS result for  $St = 0.001$ . Squares: DNS result for  $St = 0.11$ . Red-dashed-line: theory's prediction for  $St = 0.001$ . Gold-dotted-line: theory's prediction for  $St = 0.11$ . Grey-solid-line: modified-theory's prediction for  $St = 0.11$  (details of modification in the section on derivation of  $c_{st}$ ). Note: the predictions are based on the  $A_\tau$  values valid in the  $r \sim d$  regime ( $d = 9.49 \times 10^{-4}$  dm). **Inset)** Similar plots in logarithmic axes highlighting the large- $r$  regime. Note: the predictions are based on the  $A_\tau$  values valid in the  $r \gg d$  regime. It is clear that the modified-theory's predictions agree much better with the DNS.

where  $H(x)$  is the Heaviside function (zero for  $x < 0$ , unity for  $x \geq 0$ ),  $R_{f\pm}$  is the non-dimensional final position of a particle pair with an initial position of  $R_0$  and can be written as:

$$R_{f+} = R_0 \left[ \mu^2 \theta_t^2 + \frac{(1 - \mu^2)}{\theta_t} \right]^{1/2},$$

$$R_{f-} = R_0 \left[ \frac{\mu^2}{\theta_t^2} + (1 - \mu^2) \theta_t \right]^{1/2},$$

for uniaxial extension and compression respectively, where:

$$\theta_t \equiv \exp\left(\frac{t_f}{\tau_\eta \sqrt{3} f_s}\right).$$

### MRV Predictions by the Theory for Other Stokes Numbers.

As mentioned in the main text of this manuscript, even though the theory assumes that MRVs are  $St$ -independent for small  $St$ 's. Nevertheless, it could produce separate predictions for each  $St$ . Here we show the predictions for  $St = 0.001$  and  $0.11$  in Fig. 11. The prediction for  $St = 0.001$  (red dash line) agrees well with the DNS results (symbols), but the prediction for  $St = 0.11$  (gold dotted line) deviates significantly, suggesting that finite  $St$  effects not captured by the theory start to become significant and thus diminish the accuracy of the theory.

### Derivation of $c_{st}$ , its Role and Possibility of Further Corrections to The CK Theory.

In this work, we deviate crucially<sup>7</sup> from the CK theory Chun et al. (2005) by introducing an extra factor  $c_{st}$  (positive, of order unity or less) in the model of non-local diffusion:

$$q_r^D = c_{st} r \int d\Omega \int_0^\infty dt_f F(t_f) \int_{d/r}^\infty dR_0 R_0^2 \langle P \rangle(r R_0) f_I(R_0, \mu, t_f). \quad (11)$$

<sup>7</sup>'Crucial' refers to the fact that without  $c_{st}$  the theory would be inconsistent with previous experimental results (as this section will show) and it would also produces results far from our DNS results.

To determine what  $c_{st}$  is (or should be), we begin from an important finding in Chun et al. (2005) that if  $\langle P \rangle$  is power-law of  $r$ , i.e.,  $\langle P \rangle = Cr^{-c_1}$ , then the non-local diffusion  $q_r^D$  can be cast into a differential form (which is usually only true for local diffusion):

$$q_r^D = -B_{nl} \tau_\eta^{-1} r^2 \frac{\partial \langle P \rangle}{\partial r}, \quad (12)$$

where:

$$B_{nl} = \tau_\eta \int d\Omega \int_0^\infty dt_f F(t_f) \int_{d/r}^\infty dR_0 R_0^{2-c_1} f_I(R_0, \mu, t_f). \quad (13)$$

This, together with:  $q_i^d = -A_{ck} \tau_\eta^{-1} r \langle P \rangle$ , eventually leads to the first order equation differential equation for the RDF ( $g(r) \equiv V \langle P \rangle$ ), that has (only) power-law solutions:  $g(r) = VC r^{-c_1}$ . This result (i.e.,  $g(r)$  or equivalently  $\langle P \rangle(r)$  are power-laws) has seen compelling validations from both experiments (e.g., Saw et al. (2012b); Lu et al. (2010); Yavuz et al. (2018)) and DNS (e.g., Chun et al. (2005); Bec et al. (2007); Saw et al. (2012a)). We now begin from this experimentally validated result and work backward to derive an expression for  $c_{st}$ . We plug the power-law form for  $\langle P \rangle$  into (12):

$$\begin{aligned} q_r^D &= -B_{nl} \tau_\eta^{-1} r^2 \frac{\partial (Cr^{-c_1})}{\partial r} \\ &= -B_{nl} \tau_\eta^{-1} r^2 C(-c_1) r^{-c_1-1} \\ &= B_{nl} \tau_\eta^{-1} r c_1 C r^{-c_1} \\ &= \tau_\eta^{-1} r c_1 C r^{-c_1} \tau_\eta \int d\Omega \int_0^\infty dt_f F(t_f) \int_{d/r}^\infty dR_0 R_0^{2-c_1} f_I(R_0, \mu, t_f) \\ &= r c_1 \int d\Omega \int_0^\infty dt_f F(t_f) \int_{d/r}^\infty dR_0 R_0^2 C (r R_0)^{-c_1} f_I(R_0, \mu, t_f) \\ &= c_1 r \int d\Omega \int_0^\infty dt_f F(t_f) \int_{d/r}^\infty dR_0 R_0^2 \langle P \rangle(r R_0) f_I(R_0, \mu, t_f). \end{aligned}$$

Comparing with (11), we have:

$$c_{st} = | -c_1 | \equiv |c_1|,$$

which is found in experiments (and theories) to be of order 0 to 1 and a function of particle Stokes number  $St$ ; in words, this means  $c_{st}$  is given by the modulus of the power-law exponent of the RDF that would arise in the collision-less case; in the case with collision and sufficiently small particle ( $d/\eta \lesssim 1$ ), such as in this study,  $c_{st}$  equals the modulus of the power-law exponent of the RDF the range of  $d \ll r \ll 20\eta$  (note: power-laws RDF are empirically observed for  $r \ll 20\eta$  Saw et al. (2008, 2012a)). Note: we have chosen to define  $c_{st}$  using the ‘modulus’ (instead of the ‘negative’ of the power-law exponent) since it guarantees that  $q_r^D$  is negative (positive) when  $g(r)$  is an increasing (decreasing) function of  $r$ , so that we are consistent with the fact that  $q_r^D$  is a diffusion flux. We note that both the CK theory and the current modified version assume  $St \ll 1$ .

Chun et al. Chun et al. (2005) went further to provide a solution for  $c_1$  (for collision-less particles, in the  $St \ll 1$  limit):

$$c_1 = \frac{A_{ck}}{B_{nl}} \equiv \frac{A_{\tau, r \gg d} \tau_\eta}{B_{nl}}, \quad (14)$$

where we have clarified that  $A_\tau$  in our work is defined differently from "A" in (Chun et al., 2005) (we denote the latter as  $A_{ck}$  to avoid confusion), and  $A_{\tau, r \gg d}$  is our  $A_\tau$  evaluated at the large- $r$  limit. In the current context,  $c_1$  maybe obtained via (14) or alternatively directly from the power-law exponent of  $g(r)$  in the range  $d \ll r \ll 20\eta$  as discussed above. Using values of the relevant parameters in our DNS, we found  $\frac{A_\tau \tau_\eta}{B_{nl}} \approx \frac{2.4St^2 \times .0925}{.0397} = 5.6St^2$ , which is 15% smaller than the one found in Chun et al. (2005), i.e.,  $\frac{A_{ck}}{B_{nl}} \approx \frac{.61St^2}{.0926} = 6.6St^2$ . However, we have observed in our DNS that the direct method (by fitting

power-laws to the RDFs in the suitable  $r$ -range) gives  $c_1$  which is 3.2 (1.9) times larger than the one obtained using (14) for the case of  $St = 0.054$  (0.11).

A plausible interpretation of the discrepancy described just above is that there may be another missing dimensionless factor (of order unity, possibly weakly dependent on Reynolds-number) in the correct definition of  $q_r^D$ . This is beyond the scope of this present study (to avoid confusion, we currently restrict ourselves to the least speculative correction only) and is a good subject for future works. However it may be informative to note that, by inspection, we find that if we further include a factor of  $\sim 1/3$  to  $1/2$  in the definition of  $q_r^D$ , then the agreement between the theoretical (the integral version) and DNS produced  $\langle W_r \rangle$  is strikingly better in the  $r \gg d$  limit, while in the  $r \sim d$  regime, it is slightly better (the former should not come as a surprise as this is the regime of power-law RDFs and the factor of  $\sim 1/3$  is exactly designed to reproduce the correct  $c_1$ ).

To demonstrate the point just discussed, we show in Fig. 11 the predictions by the theory for the case of  $St = 0.11$ . We see that, in the  $r \sim d$  regime, the prediction by the original theory (dotted line in the main figure) is somewhat below the DNS result, while the prediction by the modified theory (with a factor of  $1/2$  appended to the definition of  $q_r^D$ ), shown as the solid line, is much closer to DNS. In the  $r \gg d$  regime, the modified theory's superiority in terms of accuracy is even more pronounced (see inset of Fig. 11).

### Relation Between $g(r)$ and $\langle P \rangle$ .

In the main text, we state that  $g(r) \equiv V \langle P \rangle$ , where  $V$  is the spatial volume of the full domain of the problem, i.e.,  $(2\pi)^3$  in the DNS. Justification: let  $g(r)$  be the ratio of probability of finding a second particle at  $r$  from a particle, to the probability of such finding in a perfectly random distributed particle population, thus:  $g(r) \equiv \frac{\langle P \rangle \delta x \delta y \delta z}{(\delta x \delta y \delta z)/V} \equiv \langle P \rangle V$ . Further, since system is isotropic,  $g(r) \equiv g(r)$ .

### Modeling of MRV based on Distribution of Particle Approach Angles $P(\theta)$ .

We imagine the particles are small, i.e.,  $d \ll \eta$  and  $St \ll 1$ . The latter implies their trajectories are almost like fluid particles', while the former implies that, viewed at the scale of interest  $r \sim d$ , their trajectories are almost rectilinear (since the radii of curvature are proportional to  $\eta$ ). Thus in the reference frame of a primary particles, no secondary particle could have a trajectory, being straight-line, that has a history of collision with the volume of the primary (otherwise coagulation would have occurred and the secondary particle in question would cease to exist). In trigonometric terms, let  $\theta$  be the angle between the secondary particle's velocity and its vector position in the rest frame of the primary particle, then we must have:  $\sin^{-1}(d/r) \leq \theta \leq \pi$ , with the convention that  $\sin^{-1}(x) \in [-\frac{\pi}{2}, \frac{\pi}{2}]$ .

From the above, we could then compute the MRV,  $\langle w_r \rangle_*$  based on fluid particles' statistics. Since collision-coagulation affects positive and negative relative particle velocities differently, we begin by writing  $\langle w_r \rangle_*$  as a sum of the positive (i.e.,  $w_r > 0$ ) and negative branches (with proper statistical weights  $p_{\pm}$  to account for possible skewness of the probability distribution of velocity):

$$\langle W_r \rangle \equiv \langle w_r \rangle_* = p_- \langle w_r | w_r < 0 \rangle_* + p_+ \langle w_r | w_r \geq 0 \rangle_* .$$

The negative branch  $p_- \langle w_r | w_r < 0 \rangle_*$  is unaffected by collision-coagulation and we thus express it as a simple linear function of  $r$  that follows from the K41-phenomenology (Kolmogorov, 1941), i.e.,  $-p_- \xi_- r$ , where  $\xi_{\pm} \sim \sqrt{\varepsilon/(15\nu)}$ ,  $\varepsilon$  is the (kinetic) energy dissipation rate of the flow. For the positive branch, we further assume that the (fluid particles') joint probability density function (PDF) of magnitude of relative velocity (secondary particle relative to primary particle)  $|\mathbf{w}|$  and approach-angle  $\theta$ ,  $P(|\mathbf{w}|, \theta)$ , is separable (note:  $w_r \equiv |\mathbf{w}| \cos(\theta)$ ), hence:

$$\begin{aligned} p_+ \langle w_r | w_r \geq 0 \rangle_* &= \int_0^{\infty} d|\mathbf{w}| \int_{\theta_m}^{\frac{\pi}{2}} d\theta P(|\mathbf{w}|, \theta) |\mathbf{w}| \cos(\theta) \\ &= \int_0^{\infty} d|\mathbf{w}| P_w(|\mathbf{w}|) |\mathbf{w}| \int_{\theta_m}^{\frac{\pi}{2}} d\theta P_{\theta}(\theta) \cos(\theta) \\ &= p_+ \int_0^{\infty} d|\mathbf{w}| P_w(|\mathbf{w}|) |\mathbf{w}| \int_{\theta_m}^{\frac{\pi}{2}} d\theta P_{\theta}^+(\theta) \cos(\theta), \end{aligned}$$

where all the  $P$ 's are PDFs, note that  $p_+ \equiv \int_0^{\frac{\pi}{2}} P_\theta d\theta$ ,  $\int_0^{\frac{\pi}{2}} P_\theta^+ d\theta \equiv \int_0^{\frac{\pi}{2}} (P_\theta/p_+) d\theta = 1$  and  $\int_0^\pi P_\theta d\theta = 1$ , also note that  $P_\theta^+ \equiv P_\theta(\theta | w_r \geq 0)$ ; more importantly  $\theta_m = \sin^{-1}(d/r)$  as previously explained. Further:

$$\begin{aligned}
& p_+ \langle w_r | w_r \geq 0 \rangle_* \\
&= p_+ \int_0^\infty d|\mathbf{w}| P_w(|\mathbf{w}|) |\mathbf{w}| \int_{\theta_m}^{\frac{\pi}{2}} d\theta P_\theta^+(\theta) \cos(\theta) \\
&= p_+ \int_0^\infty d|\mathbf{w}| P_w(|\mathbf{w}|) |\mathbf{w}| \left[ \int_0^{\frac{\pi}{2}} d\theta P_\theta^+(\theta) \cos(\theta) + \int_{\theta_m}^0 d\theta P_\theta^+(\theta) \cos(\theta) \right] \\
&= p_+ \int_0^\infty d|\mathbf{w}| P_w(|\mathbf{w}|) |\mathbf{w}| \int_0^{\frac{\pi}{2}} d\theta P_\theta^+(\theta) \cos(\theta) \left[ 1 + \frac{\int_{\theta_m}^0 d\theta P_\theta^+(\theta) \cos(\theta)}{\int_0^{\frac{\pi}{2}} d\theta P_\theta^+(\theta) \cos(\theta)} \right] \\
&= p_+ \xi_+ r \left[ 1 + \frac{\int_{\theta_m}^0 d\theta P_\theta^+(\theta) \cos(\theta)}{\int_0^{\frac{\pi}{2}} d\theta P_\theta^+(\theta) \cos(\theta)} \right],
\end{aligned}$$

where in the last line, we have replaced the first two integrals, combined, with its K41 estimate, where  $\xi_\pm \sim \sqrt{\varepsilon/(15\nu)}$ .

### Prediction of the Peak Location of the RDF Using the Differential Form of the Drift-Diffusion Equation.

$$-\tau_\eta^{-1} B_{nl} r^4 \frac{\partial g}{\partial r} + g(r) [r^2 \langle W_r \rangle - A_\tau r^3] = -R_c^*, \quad (15)$$

A finite  $R_c^*$  inhibit us from locating the peak of the RDF using (15) à la Lu et al. (2010) i.e., without knowing  $g(r)$ , since  $g(r)$  could no longer be factored out when  $\frac{\partial g}{\partial r} = 0$ . However, we argue that (15) could still give a reasonably accurate account of the peak location. For the case of  $St = 0.05$ , at  $r = 3d$  (the approximate peak location), we found the DNS data gives  $-\tau_\eta B_{nl} r^4 \frac{\partial g}{\partial r} \Big|_{\approx 0} + g(r) [r^2 \langle W_r \rangle - A_\tau r^3] \approx -1.05 \times 10^{-9}$  and  $-R_c^* \approx -1.01 \times 10^{-9}$

### General Analytical Solution for the Differential Form of the Drift-Diffusion Equation.

The general solution for the first-order non-homogenous ordinary differential equation (see, e.g., Arfken and Weber (1999)), with  $\langle w_r \rangle_*$  given by the model in the main text, is:

$$g(r) = \frac{1}{\beta(r)} \left[ \int \beta(r) q(r) dr + C \right], \quad (16)$$

with  $q(r) = R_c^*/(\tau_\eta B_{nl} r^4)$ ;  $\beta(r) = \exp \left[ \int p(r) dr \right]$  and  $p(r) = [A_\tau r - \langle w_r \rangle_*] / (\tau_\eta B_{nl} r^2)$ . For the current model described in the main text, the integral in (16) could not be expressed in terms of simpler canonical functions. Hence, for specific applications, we currently anticipate that some sort of power-law expansion or asymptotic reduction (if not numerical integration) would be needed to produce problem specific analytical approximations.

### Further Details on the Effects of Gravity.

We repeat the DNS case of  $St = 0.054$  and  $St = 0.54$  with the particles subjected to gravity (body force), and compares results with the zero-gravity case. Fig. 12 shows the results for case  $St = 0.054$ . There is no discernible difference between the cases with and without gravity.

For case  $St = 0.54$ , the main RDF and MRV results is shown the main text. Here we show only the compensated-RDFs ( $g_c(r)$ ), where each  $g_c(r)$  is calculated via  $g(r)$  divide by a power law ( $c_0 r^{-c_1}$ ) that resulted from curve-fitting to the original  $g(r)$  in the range  $0.6\eta \leq r \leq 3\eta$ . Fig. 13 compares  $g_c(r)$  for cases with and without gravity. The fact that there is no discernible difference implies that the uncompensated  $g(r)$  could be model as  $g_c \times g_g$  where  $g_c$  is function that depends only on the particle collision process while  $g_g$  depends on other factors, e.g., gravity and is independent of particle collision.

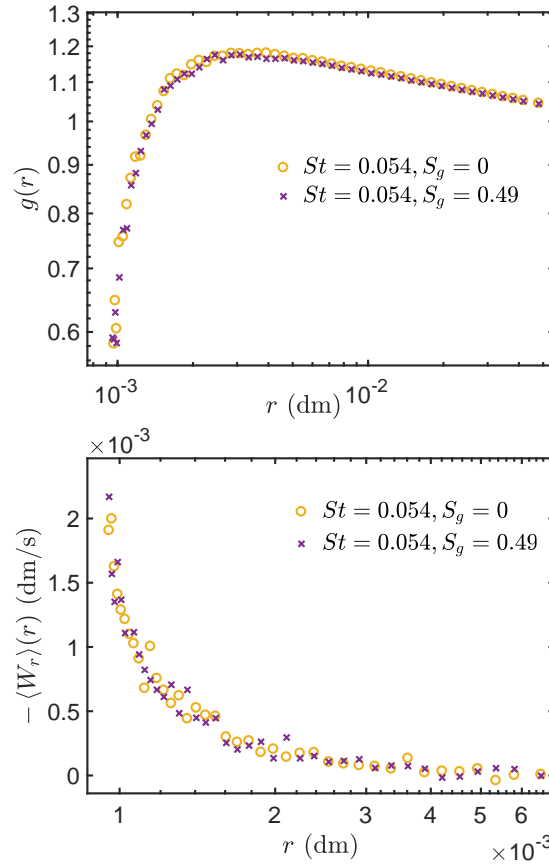


**Figure 12. Top** RDFs of particles ( $St = 0.054$ ) subject to action of turbulence, collision-coagulation with and without gravity. Circles:  $S_g = 0$  (zero gravity); triangles:  $S_g = 0.49$  (nonzero gravity). No discernible effect of gravity. **Bottom** MRVs of the same cases. No discernible effect of gravity.

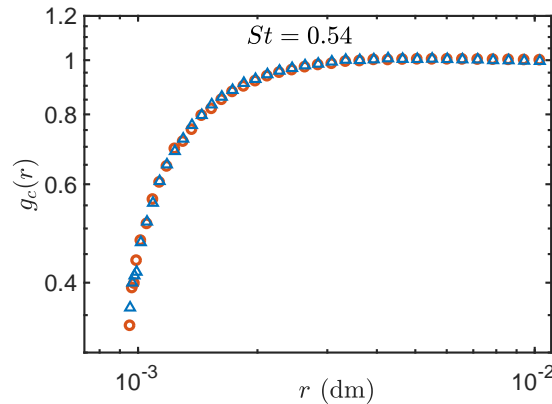


**Figure 13.** Compensated RDFs of particles ( $St = 0.54$ ) subject to action of turbulence, collision-coagulation with and without gravity. Circles:  $S_g = 0$  (zero gravity); triangles:  $S_g = 4.9$  (nonzero gravity). Interpretation in the text.